

Article

A Selective Fluorescent Optode for Lead(II) Based on the Dansylamidopropyl Pendant Arm Derivative of 1,4-Dioxa-7,13-dithia-10-azacyclopentadecane ([15]aneNS₂O₂)

Mojtaba Shamsipur^{1,*}, Moslem Mohammadi¹, Massimiliano Arca² , Alessandra Garau² , Vito Lippolis^{2,*}  and Ali Barati¹

¹ Department of Chemistry, Razi University, Kermanshah, Iran; m.mohammadi@yahoo.com (M.M.); alibarati@razi.ac.ir (A.B.)

² Dipartimento di Scienze Chimiche e Geologiche, Università degli Studi di Cagliari, S.S. 554 Bivio per Sestu, 09042 Monserrato, CA, Italy; marca@unica.it (M.A.); agarau@unica.it (A.G.)

* Correspondence: mshamsipur@yahoo.com or m.shamsipur@razi.ac.ir (M.S.); lippolis@unica.it (V.L.)

Abstract: In this study, a novel highly sensitive and selective fluorescent optode membrane aimed at the determination of Pb(II) ion is proposed by incorporating *N*-(3-(1,4-dioxa-7,13-dithia-10-azacyclopentadecan-10-yl)propyl)-5-(dimethylamino)naphthalene-1-sulfonamide (L) as fluoroionophore in polyvinyl chloride (PVC) containing 2-nitrophenyl octylether (NPOE) as a plasticizer. In addition to high stability and reproducibility, the proposed optosensor showed a unique selectivity toward Pb(II) ion, with a wide linear range of molar concentrations (1.0×10^{-9} – 1.0×10^{-3} M) and a low detection limit of 7.5×10^{-10} M in solution at pH 5.0. The formation constants of the Pb(II) complexes with the fluoroionophore were evaluated by fitting the fluorescence data with a nonlinear least-squares curve-fitting program, and further information about the structures of the complexes were evaluated based on hybrid-DFT calculations. The optosensor exhibited a fast response time of less than three min, being easily regenerated by exposure to a solution of dithiothreitol. The sensor was applied to the determination of Pb(II) in real samples (canned tuna fish), and it provided satisfactory results comparable to those obtained via atomic absorption spectrometry (AAS).

Keywords: optical sensor; macrocyclic ligands; lead; PVC membrane; fluorescence spectroscopy



Citation: Shamsipur, M.; Mohammadi, M.; Arca, M.; Garau, A.; Lippolis, V.; Barati, A. A Selective Fluorescent Optode for Lead(II) Based on the Dansylamidopropyl Pendant Arm Derivative of 1,4-Dioxa-7,13-dithia-10-azacyclopentadecane ([15]aneNS₂O₂). *Chemosensors* **2023**, *11*, 571. <https://doi.org/10.3390/chemosensors11120571>

Academic Editor: Ambra Giannetti

Received: 16 October 2023

Revised: 14 November 2023

Accepted: 28 November 2023

Published: 1 December 2023



Copyright: © 2023 by the authors. Licensee MDPI, Basel, Switzerland. This article is an open access article distributed under the terms and conditions of the Creative Commons Attribution (CC BY) license (<https://creativecommons.org/licenses/by/4.0/>).

1. Introduction

The increasing presence of heavy metal ions such as Cd(II), Pb(II), and Hg(II) in the environment is the reason behind growing public concern due to their adverse effects on human health under intoxication conditions [1]. Lead(II) is one of the most toxic heavy metal ions, and its presence in the environment is continuously increasing due to its usage in many industrial processes and human activities [2]. Prolonged exposure to this metal ion can cause numerous pathological diseases and metabolic disorders, including carcinogenicity, muscle paralysis, memory loss, and mental retardation [3]. Therefore, increasingly reliable, sensitive, and selective probes, and analytical methods are continuously required for monitoring and assessing lead(II) levels in environmental matrices and living organisms. Several methods can be used for measuring the level of Pb(II) in real samples, including voltammetry [4], ICP-AES [5], ICP-AMS [6], flame atomic absorption spectrometry [7], graphite furnace atomic absorption spectrometry [8], and spectrophotometry [9]. Although these analytical techniques are sensitive and accurate, they generally require costly measuring equipment, qualified personnel, laborious sample pre-treatment, and they cannot be considered for in-field and on-line analysis. On the contrary, among other screening methods available, those based on the use of optical sensors represent a valid alternative in terms of simplicity and sensitivity for the rapid monitoring of lead(II) and other toxic metal ions in environmental and biological matrices. In particular, fluorescent chemosensors [10]

seem to be ideal tools because fluorescence measurements are sensitive, low-cost, and the sample preparation is simple and not necessarily disruptive. In addition, fluorescence spectroscopy offers the possibility of local observation in cells and tissues using microscopy techniques. During the past 15–20 years, many research groups have been engaged in research programs devoted to the use of medium-sized macrocyclic ligands featuring different donor atoms, ring size cavity and molecular structure, for the development of optically selective fluorescent chemosensors for either essential to human life metals, i.e., Mg(II), Zn(II) or toxic heavy metals (Cd(II), Pb(II), Hg(II)), following synthetic paradigms based on the principles of supramolecular chemistry [11–28]. In general, fluorescent chemosensors for metal ions consist of a receptor unit (for example a macrocyclic ligand) covalently linked through a spacer to a fluorogenic unit (conjugated fluorescent chemosensors) so that the selective host–guest interaction in solution of the target species at the receptor site is converted into a selective enhancement or quenching of the fluorophore emission signal, which can be easily detected. This supramolecular scheme could be translated into an operative synthetic approach: “find the appropriate receptor and link a fluorogenic fragment to it”. This approach has worked particularly well with crown ethers for the development of fluorescent chemosensors for alkaline metal cations [10]. However, the design of highly selective binding units is a very challenging task, and the signaling unit could also be involved in the target species binding process (i.e., the fluorophore features coordinating donor atoms). In this case the optical selectivity (a change in the fluorescence emission intensity is observed only in the presence of one species) could be achieved even in the absence of thermodynamic or binding selectivity (more than one species can bind equally efficiently the molecular chemosensor). This is still a favorable situation as thermodynamic selectivity could be reached by changing the host–guest interaction medium, for example, it has been shown that selectivity in the binding process can be achieved once the chemosensor is dispersed in polyvinyl chloride (PVC), where other factors such as mobility and lipophilicity come into action [11,14–16,18]. Furthermore, for many analytical applications, binding selectivity of the chemosensor is not strictly necessary either because the absence of binding-interfering species in the sample considered is known or only a quick qualitative response is required about the presence of the target species in the analyzed matrix. This makes the quest for optical selectivity a priority for an optical chemosensor as compared to binding selectivity, thus rendering the molecule design and synthesis easier. Of course, a chemosensor featuring the selectivity of both would represent the best situation.

Following our interest in this field (particularly in the use of macrocyclic ligands as receptor units according to the above-mentioned receptor–spacer–fluorophore supramolecular scheme), in the present study, the suitability of the dansylamidopropyl pendant arm derivative of the mixed-donor macrocycle 1,4-dioxa-7,13-dithia-10-azacyclopentadecane ([15]aneNS₂O₂), i.e., *N*-(3-(1,4-dioxa-7,13-dithia-10-azacyclopentadecan-10-yl)propyl)-5-(dimethylamino)naphthalene-1-sulfonamide (**L**, Figure 1), for the preparation of a selective polyvinyl chloride (PVC)-based Pb(II) fluorescent optode membrane was examined, and the concentration of Pb(II) in authentic samples was satisfactorily determined with the new membrane sensor.

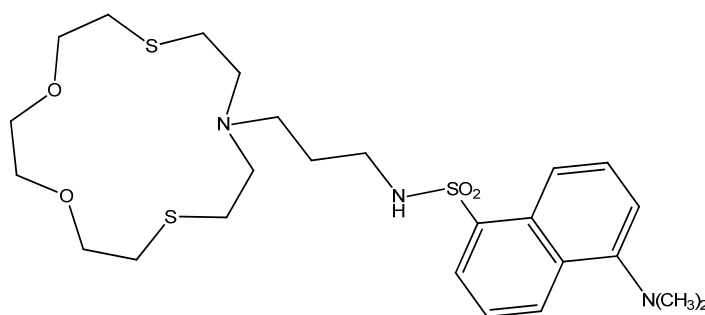


Figure 1. *N*-(3-(1,4-dioxa-7,13-dithia-10-azacyclopentadecan-10-yl)propyl)-5-(dimethylamino)naphthalene-1-sulfonamide (**L**).

2. Materials and Methods

2.1. Reagents and Apparatus

All chemicals used (metal cations as nitrate salts) including solvents and polyvinyl chloride (PVC) of high relative molecular weight were analytical reagent-grade (Sigma or Merck) and were used without any further purification. Among the chemicals used, 2-nitrophenyl octylether (NPOE) was purchased from Acros. Doubly distilled water was used throughout. *N*-(3-(1,4-dioxo-7,13-dithia-10-azacyclopentadecan-10-yl)propyl)-5-(dimethylamino)naphthalene-1-sulfonamide (**L**) was synthesized according to the procedure reported in the literature [29]. A Varian Cary Eclipse fluorescence spectrometer was used for the fluorescence measurements, while the pH measurements were carried out on a Metrohm 692 pH/ion meter.

2.2. Procedure for the Determination of Pb(II) in Canned Tuna Samples

About 10.0 g of canned tuna samples were placed in a crucible and were dried at 100 °C for 24 h. The dried samples were ashed in a furnace at 550 °C. Subsequently, 5 mL of a HNO₃/HCl, 1:3 (*v/v*) solution was added, and the mixtures were heated until dissolution was completed. The solutions were then cooled and completely transferred to a calibrated 50 mL volumetric flask. The pH of the solutions was adjusted to 5.0 (see Section 3.4) by an acetate buffer. Proper sample solutions were prepared by appropriately diluting the mother solution with doubly distilled water. The lead(II) content of the sample was determined using the standard addition method [30].

2.3. Optode Membrane Preparation

PVC-based optode membranes for Pb(II) sensing were prepared by mixing 5 mg of **L**, 5 mg of sodium tetraphenylborate (NaTPB), 30 mg of polyvinyl chloride (PVC) powder, and 60 mg of 2-nitrophenyl octylether (NPOE), and dissolving the obtained mixture in 2 mL of THF. Of the homogenized solution, 0.2 mL was cast onto glass plates (28 mm × 13 mm × 1 mm) and spread by using a spin-on device (2600 rpm rotation frequency, about 15 s spinning time). The obtained optode was kept in ambient air for 1 h before use. The supported membranes, obtained from the previous steps, were placed in a diagonal position in the quartz cell (10 mm × 10 mm × 50 mm dimensions) containing 2.0 mL of an acetate buffer solution (pH 5.0, see Section 3.4). A membrane, not containing **L**, was tested as the blank membrane. Before the first measurement of Pb(II) ion was made, the membrane was soaked for more than 20 min, until a stable fluorescence response was revealed. The sensor was excited at 342 nm to measure its fluorescence intensity at 520 nm. During titrations with a standardized solution of Pb(II), the fluorescence intensity of the optode was measured after adequate time (3 min) to ensure that the equilibrium was reached. The limit of detection of the optimized membrane was estimated as the [Pb(II)] producing an analytical signal equal to three times the standard deviation of the signal recorded for the blank.

2.4. Theoretical Calculations

Theoretical calculations were performed at the density functional theory (DFT) [31] level on Pb(II), **L**, [Pb(**L**)]²⁺, and [Pb(**L**)₂]²⁺ with the Gaussian 16 [32] commercial suite. Based on a previous validation carried out on strictly related compounds [33], the mPW1PW hybrid functional [34] was adopted in combination with the Ahlrichs split-valence basis sets (BSs) in the Weigend's formulation (def2SVP) [35], featuring relativistic effective core potentials (RECPs) for the heavier Pb atom. Fine numerical integration grids were adopted. Harmonic frequency calculations were used to verify the nature of the minima of the optimized structures and carry out thermochemical analysis (Tables S1–S5). A population analysis at the NBO level [36,37] was carried out, and Wiberg bond indexes [36] were calculated at the optimized geometries. The optimized geometries and the isosurfaces of KS-MOs were investigated using the GaussView 6.0.16 [38] and Molden 7.2 [39] programs.

3. Results and Discussion

3.1. Preliminary Studies

Initially, we performed the titration of MeCN solutions of **L** with different metal ions, including Pb(II). The variations in the excitation and emission fluorescence spectra were recorded upon the addition of an increasing amount of Pb(II) (Figure 2) and other selected metal cations (Figure 3) to acetonitrile (MeCN) solutions of the ligand (5.0×10^{-5} M) at 25.0 ± 0.1 °C. As seen in Figure 2, the emission spectra of the ligand show a sharp band at 518 nm, which significantly decreased as a function of the [Pb(II)]/[L] molar ratio (to underline the importance of the medium in which the host–guest binding process takes place, it is important to consider that in MeCN/H₂O (4:1 *v/v*) at pH 7.0, the optical response of **L** to the presence of Pb(II) could not be studied due to the formation of an insoluble precipitate [29]). The quenching effect is smaller for the other metal cations considered, with changes in the emission spectrum of **L** upon titration with these metals that are similar to those observed in the case of the titration with Pb(II) (Figure 2). The corresponding plots of the fluorescence intensity at the maximum emission wavelength as a function of the [Pb(II)]/[L] ratio (Figure 3), show two distinct inflection points at [Pb(II)]/[L] ratios of 0.5 and 1.0, presumably attributable to the formation of both [Pb(L)₂]²⁺ and [Pb(L)]²⁺ complex cations. The plots in Figure 3 were confirmed by repeated titration experiments.

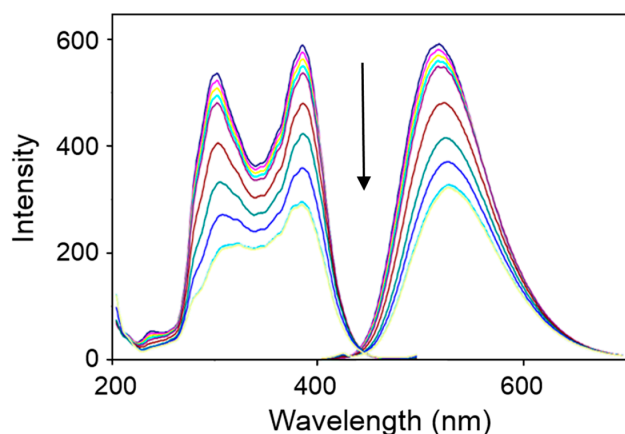


Figure 2. Excitation (left) and emission (right) spectra of **L** in a MeCN solution at 25.0 ± 0.1 °C during a spectrofluorimetric titration in the presence of increasing concentrations of Pb(II). [L] = 5.0×10^{-5} M. The [Pb(II)]/[L] molar ratio corresponding to each of the 10 spectra reported (from up to down) is shown in Figure 3 in correspondence with the first 10 points in the titration plot with Pb(II) (from left to right).

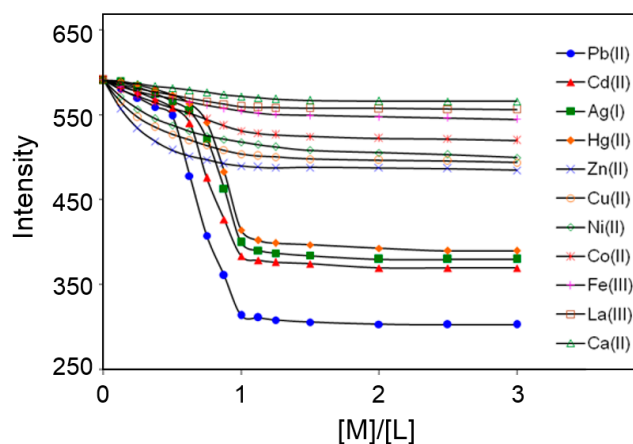


Figure 3. Plots of the fluorescence intensity as a function of the [M]/[L] molar ratio during a spectrofluorimetric titration of **L** with various metal ions in the MeCN solution at 25.0 ± 0.1 °C. [L] = 5.0×10^{-5} M. In the case of Pb(II), the emission spectrum recorded in correspondence with each of the first 10 points (from left to right) in the titration plot is shown in Figure 2 (from up to down).

The formation constants of these two complexes and those regarding the complexation of the other metal cations considered were calculated by applying a nonlinear least-squares curve-fitting model [40,41] (Table 1) to the fluorescence intensity versus $[M]/[L]$ ratio data.

Table 1. Formation constants ($\log K$) calculated for the complexes of different metal ions, M, with the ligand L in MeCN.

Metal	$\log K$	
	M(L)	M(L) ₂
Pb(II)	11.27 ± 0.05	4.61 ± 0.03
Hg(II)	7.63 ± 0.04	4.08 ± 0.04
Ag(I)	7.86 ± 0.04	4.21 ± 0.03
Cd(II)	8.39 ± 0.05	4.49 ± 0.05
Fe(III)	3.72 ± 0.03	---
Co(II)	4.11 ± 0.05	---
Ni(II)	4.59 ± 0.03	---
Cu(II)	5.22 ± 0.04	---
Zn(II)	5.71 ± 0.03	---
La(III)	3.56 ± 0.05	---
Ca(II)	3.04 ± 0.04	---

The results discussed above supported the formation of the most stable Pb(II) complexes in the series followed by Cd(II), Ag(I) and Hg(II), which also form both $[M(L)]^{2+}$ and $[M(L)_2]^{2+}$ complexes. Further information about the structures of the fluorophore L and its Pb(II) complexes were obtained from hybrid DFT [31] gas phase calculations (Figure 4).

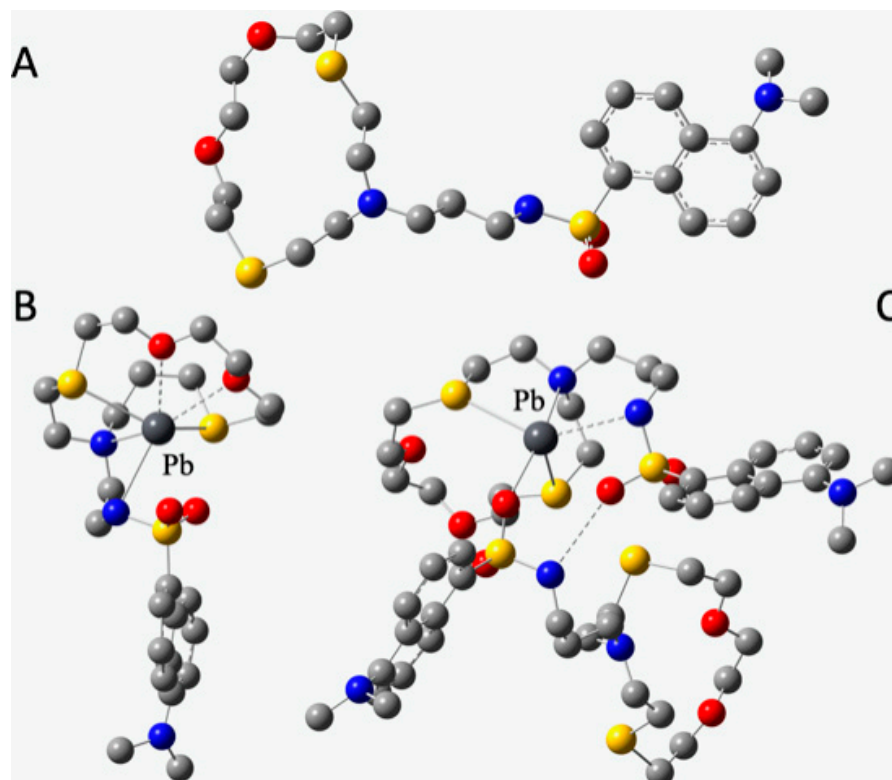


Figure 4. Optimized structures of the ligand L (A) and the complexes $[Pb(L)]^{2+}$ (B), and $[Pb(L)_2]^{2+}$ (C). Legend: gray (C); blue (N); red (O); yellow (S); dark gray (Pb). Hydrogen atoms were omitted for clarity.

In the optimized structure of the 1:1 $[Pb(L)]^{2+}$ complex (Figure 4B), the cation is well-incorporated inside the cavity of the twisted macrocyclic framework and coordinated by all the donor atoms of the ligand molecule (five atoms from the macrocyclic moiety and

the amidic N-donor atom), analogously to what is found in related metal complexes [42]. The Pb–O (2.783 and 2.794 Å), Pb–S (2.946 and 2.975 Å), and Pb–N (Pb–N_{macro} = 2.687; Pb–N_{amid} = 2.854 Å) are all longer than the sum of the corresponding covalent radii. Accordingly, the large natural charge [37] on the metal ion ($Q_{\text{Pb}} = 1.185 |e|$) and the modest Wiberg [36] bond indexes (average $\text{WBI}_{\text{Pb-O}} = 0.10$; $\text{WBI}_{\text{Pb-S}} = 0.29$; $\text{WBI}_{\text{Pb-N}} = 0.18$ and 0.11 for the macrocyclic and amidic nitrogen atoms, respectively) suggest a prevalently electrostatic interaction between the metal ion and the coordinating ligand atoms. This notwithstanding, it is worth noting that a second-order perturbation analysis (SOPTA) of the Fock matrix in the NBO basis indicates an intramolecular interaction of 22.6 kcal/mol from the amidic nitrogen atom to the lead(II) ion.

In the optimized structure of the 1:2 $[\text{Pb}(\text{L})_2]^{2+}$ complex (Figure 4C), the Pb(II) ion is coordinated by two S-atoms (2.780 and 2.972 Å) and an N-atom of the macrocycle of one ligand unit (2.687 Å) and the amidic nitrogen of the second ligand (2.854 Å). The coordination is supported by one short Pb–O interaction (2.429 Å) from the sulfone moiety. The two macrocycles are further connected by a hydrogen bond involving the amidic N–H group of a ligand and the sulfone group of the other. Of note, the interaction between the amidic nitrogen and the lead(II) ion involves only one of the two ligand units with a lower energy (14.46 kcal/mol; $\text{WBI}_{\text{Pb}\cdots\text{N}} = 0.079$) that was evaluated via SOPTA analysis.

The lower number of interactions with the macrocyclic moieties in the 1:2 complex with respect to those in the 1:1 complex is reflected in a remarkable lowering of the stabilization energies resulting from the formation of the 1:1 complex (from the ligand and the free Pb(II) ion; $\Delta E_1 = 257.61$ kcal/mol; Table S1) as compared to the formation of the 1:2 complex (from the ligand and the 1:1 complex; $\Delta E_2 = 33.54$ kcal/mol; Table S1). Accordingly, the same trend was calculated for the reaction free energy variations related to the 1:1 and 1:2 complex formation ($\Delta G_1 = -241.4$; $\Delta G_2 = -17.2$ kcal/mol; Table S1). This may tentatively justify the significantly lower formation constant evaluated experimentally in MeCN for $[\text{Pb}(\text{L})_2]^{2+}$ compared to $[\text{Pb}(\text{L})]^{2+}$ (Table 1). The involvement of the amidic N atom(s) in the metal coordination, both in the 1:1 and, to a lesser extent, 1:2 Pb(II)/L complexes, might account for the quenching effect observed in the solution. The lower N–Pb(II) interaction energy, as well as the smaller N–Pb bond orders in the 1:2 complex compared to the 1:1 complex, are in agreement with the lower quenching observed in the former case compared to the latter (Figure 3). On the basis of these results, we expected L to be suitable for the preparation of a PVC optode selective for Pb(II), considering also that once incorporated in plasticized PVC, the optical and binding selectivity of the chemosensor could improve. In fact, other factors such as mobility and lipophilicity of the different species participating in the binding/signaling event could have some effects in this respect [11,14–16,18] (see Section 1).

3.2. Operation Principle

The membrane optical sensor was prepared by incorporating L and sodium tetraphenylborate (NaTPB) as a lipophilic anionic additive in plasticized PVC. TPB[−] provides the necessary ion exchange properties for the optode membrane; this is necessary because L is neutral and cannot behave as an ion exchanger [14], according to the heterogeneous equilibrium (1):

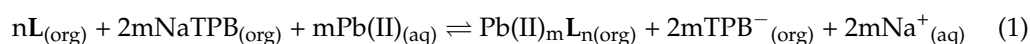


Figure 5A shows changes in the excitation (left) and emission spectra (right) of the Pb(II) optode membrane at the optimized composition (see Section 3.3) upon increasing the concentrations of the Pb(II) ion (all measurements were obtained at pH = 5.0 (see Section 3.4), adjusted with an acetate buffer). A decrease in both the excitation and emission intensities was observed upon increasing the concentration of Pb(II). Based on the experimental response of the optode membrane, the following theoretical measuring model for the determination of Pb(II) can be proposed [14]. The overall equilibrium between Pb(II) in the

aqueous solution ($\text{Pb(II)}_{(\text{aq})}$) and L in the plasticized PVC membrane organic phase ($\text{L}_{(\text{org})}$) to afford a $\text{Pb(II)}_m\text{L}_n$ complex can be represented as follows:



with the constant for the overall reaction given by (3):

$$\beta = [\text{Pb(II)}_m\text{L}_n]_{(\text{org})} / [\text{Pb(II)}]_{(\text{aq})}^m [\text{L}]_{(\text{org})}^n \quad (3)$$

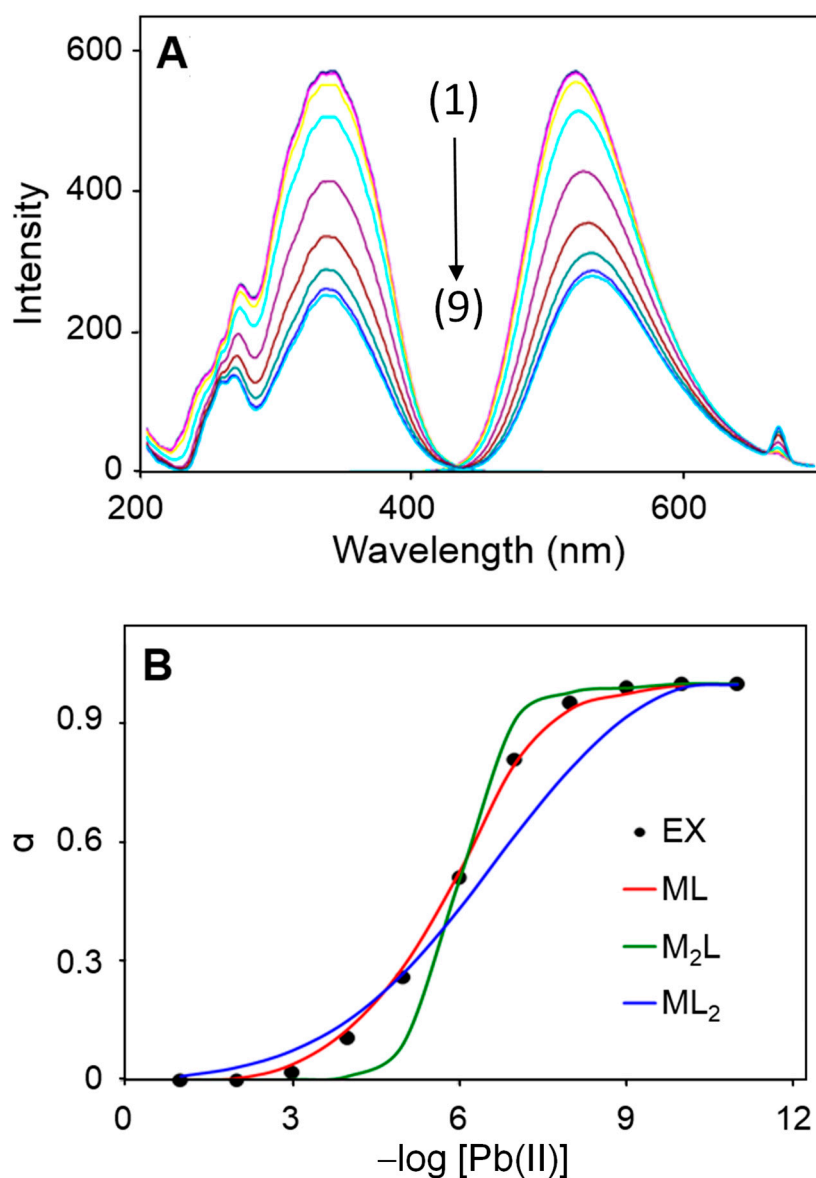


Figure 5. Changes in the excitation (left) and emission spectra (right) of the Pb(II) optode membrane at the optimized composition upon increasing the concentrations of the Pb(II) ion (A) (all measurements were obtained at pH = 5.0 (see Section 3.4), adjusted with an acetate buffer): (1) solution of L , (2) 1.0×10^{-9} M, (3) 1.0×10^{-8} M, (4) 1.0×10^{-7} M, (5) 1.0×10^{-6} M, (6) 1.0×10^{-5} M, (7) 1.0×10^{-4} M, (8) 1.0×10^{-3} M, (9) 1.0×10^{-2} M (Pb(II) solutions that were more diluted than 10^{-9} M and more concentrated than 10^{-2} M, showed emission spectra superimposable to those recorded for the 10^{-9} and 10^{-2} M solutions, respectively); α (see Equation (5)) as a function of $-\log[\text{Pb(II)}]$ (B). The fitting of the experimental data (black dots) was performed using Equation (6): $m:n = 1:1$ (red curve), $m:n = 1:2$ (blue curve), $m:n = 2:1$ (green curve).

The relative fluorescence intensity is defined by the ratio between the uncomplexed **L** in the organic phase ($[L]_{(org)}$) and its total amount ($[L_{tot}]_{(org)}$):

$$\alpha = [L]_{(org)}/[L_{tot}]_{(org)} \text{ and } [Pb(II)_m L_n]_{(org)} = [L_{tot}]_{(org)} (1 - \alpha)/n \quad (4)$$

The value of α during titration with Pb(II) can be evaluated by measuring the fluorescence intensity of the optode membrane, FI, according to (5):

$$\alpha = (FI - FI_t)/(FI_0 - FI_t) \quad (5)$$

In Equation (5), FI_t and FI_0 are the fluorescence intensities of the optode in the limit situations of **L** that is totally complexed ($\alpha = 0$) and totally uncomplexed ($\alpha = 1$), respectively.

By combining Equations (3) and (4), we can obtain the relationship between α and $[Pb(II)]$ in water solution:

$$(1 - \alpha)/\alpha^n = n \beta [L_{tot}]_{(org)}^{n-1} [Pb(II)]_{(aq)}^m \quad (6)$$

Equation (6) can be used for the quantitative determination of Pb(II) using the proposed optode membrane.

3.3. Optimization of the Membrane Composition

The effect of the membrane composition [43–47] on the response of the optode to Pb(II) was tested by preparing different membranes featuring different types of plasticizer, the nature of which can significantly influence both the measuring concentration range and the selectivity coefficients [45–47]. Different molar concentrations of **L** and NaTPB as a lipophilic anionic additive necessary to facilitate the ion exchange equilibrium between the membrane and the sample [46,47] (Table 2) were tested, while keeping the plasticizer/PVC ratio in the recommended range of 1.6–2.2 [15,45].

Table 2. Optimization of the membrane composition ^a.

Membrane No.	PVC/mg	Plasticizer/mg	NaTPB/mg	L/mg	Dynamic Range/M
1	30	60(NPOE)	5	5	1.0×10^{-9} – 1.0×10^{-3}
2	30	60(TEHP)	5	5	2.5×10^{-8} – 1.0×10^{-4}
3	30	60(DOS)	5	5	5.0×10^{-7} – 5.0×10^{-5}
4	30	60(DOP)	5	5	1.0×10^{-8} – 5.0×10^{-4}
5	30	60(DBP)	5	5	1.0×10^{-7} – 5.0×10^{-5}
6	31	60(NPOE)	5	4	2.5×10^{-8} – 2.5×10^{-4}
7	29	60(NPOE)	5	6	5.0×10^{-8} – 5.0×10^{-4}
8	31	60(NPOE)	4	5	7.5×10^{-8} – 2.5×10^{-4}
9	29	60(NPOE)	6	5	5.0×10^{-8} – 7.5×10^{-4}
10	35	60(NPOE)	5	0	1.0×10^{-5} – 1.0×10^{-4}

^a Polyvinyl chloride (PVC), 2-nitrophenyl octylether (NPOE), tris(2-ethylhexyl)phosphate (TEHP), dioctylsebasate (DOS), dioctylphthalate (DOP), dibutylphthalate (DBP), sodium tetraphenylborate (NaTPB).

The use of NPOE resulted in the largest measuring range (see membranes No. 1 and No. 6–9 in Table 2). An amount of 5 mg of **L** in the PVC–membrane afforded the best response of the selective sensor to Pb(II). Therefore, membrane No. 1 with the optimized PVC/NPOE/NaTPB/**L** wt% ratio of 30:60:5:5 was selected for further studies.

3.4. Effect of pH of the Test Solution on the Response of the Optode to Pb(II)

The effect of varying the acidity of test solutions on the optical response of the optode membrane at the optimized composition is shown in Figure 6. Fluorescence intensity measurements were carried out in the pH range 2–9 (the pH value was adjusted with diluted solutions of either NaOH or HNO₃) for 1.0×10^{-6} M solutions of Pb(II). The fluorescence intensity increases with the pH, reaching the maximum value at pH 5.0 (Figure 6). The lower response of the chemosensor at pH < 4 could be determined by the protonation of the nitrogen atoms of **L** and consequent extraction of H⁺ from the test solution into the membrane. On the other hand, on increasing the pH value, a swelling

of the polymeric membrane could occur, as well as formation of the hydroxo species of lead(II) [14–16,18]. All measurements with the membrane at the optimized composition were, therefore, performed in solutions buffered at pH = 5.0 with an acetate buffer.

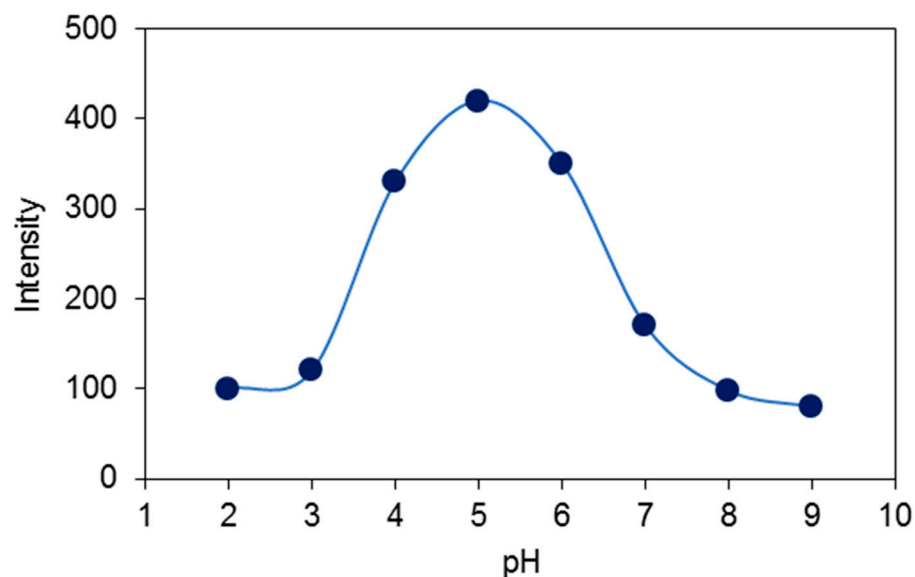


Figure 6. Fluorescence response of the optode membrane at the optimized composition (see Section 3.3) in the presence of 1.0×10^{-6} M Pb(II) ion on changing the pH of the test solutions.

3.5. Dynamic Range and Limit of Detection

Figure 5B shows the fluorescence response of the Pb(II) optode membrane at the optimized composition on varying the concentration of Pb(II) in solution buffered at pH = 5.0 (see Section 3.4).

Based on Equation (6), three fitted curves were obtained for different m:n ratios (Figure 5B). The curve for the formation of the 1:1 $[\text{Pb(L)}]^{2+}$ complex ratio fits best to the experimental data with an appropriate K value of 1.42×10^7 . This curve can be used as a calibration curve for the determination of the concentration of Pb(II) ions in a range between 1.0×10^{-9} and 1.0×10^{-3} M. The limit of detection resulted in 7.5×10^{-10} M.

3.6. Response Time, Regeneration, Short-Term Stability, and Selectivity

The dynamic response time of the optode at the optimized composition was estimated by plotting the fluorescence intensity emission versus time upon gradually changing the concentration of Pb(II) from 10^{-8} to 10^{-4} M at pH = 5.0, and recording the emission spectrum every 3 min. The resulting intensity–time curve (Figure S1) reveals that no more than 3 min are indeed necessary for the optode to reach its equilibrium response within the $[\text{Pb(II)}]$ range considered. However, the fluorescence signal of the optode membrane did not completely recover upon switching the concentration of Pb(II) back from high to low values. Despite this undesirable drawback, it was found that the fluorescence signal was fully recovered to the initial emission intensity (superimposable spectra) after immersion of a used optode in a 1.0×10^{-3} M dithiothreitol solution for one minute, following the complete stripping of Pb(II) from the membrane.

The optical membrane was also kept in contact for 2 h with a 1.0×10^{-6} M solution of Pb(II) buffered at pH 5.0 in order to study its short-term stability. The fluorescence emission intensity was regularly recorded over this period time every 15 min, and no evidence of leakage of L from the optode was observed.

The repeatability was evaluated by measuring the Pb(II) concentration with the same single optode for five repeated determinations (a regeneration with dithiothreitol of the optode was performed before each measurement). Relative standard deviations (RSD) of 2.2% and 2.0% were obtained for the 1.0×10^{-6} and 1.0×10^{-8} M Pb(II) solutions,

respectively. On the other hand, the reproducibility was evaluated by preparing five different membranes with the same composition, and measuring for each one of them the fluorescence emission intensity in a 1.0×10^{-6} M solution of Pb(II) (five repeated determinations) buffered at pH 5.0. The coefficient of variation was found to be $\pm 2.8\%$. Overall, the optode was found to be stable over a period of 3 months when not in use and kept in air, the fluorescence signal value remaining unchanged.

The selectivity of the optical membrane (i.e., the influence on the fluorescence response of the optode recorded for Pb(II) in the presence in solution of other possible interfering common metal cations) was also investigated (Figure 7).

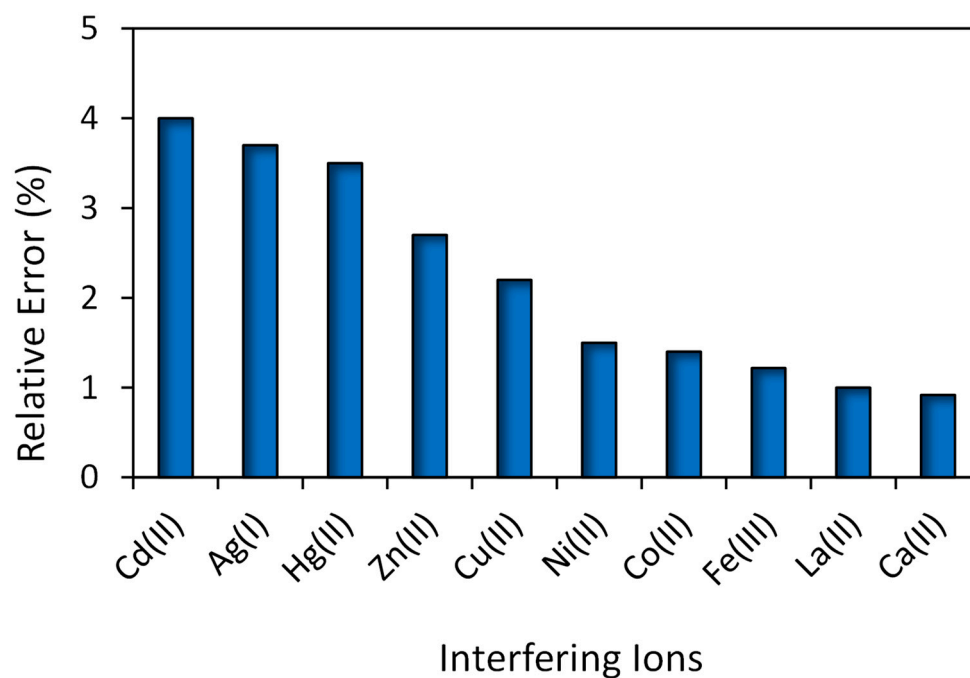


Figure 7. Interference of different cations (1.0×10^{-4} M) in the fluorescence determination of Pb(II) ion (1.0×10^{-6} M) with the proposed optode sensor.

In particular, the concentration of Pb(II) was fixed at 1.0×10^{-6} M in solutions buffered at pH = 5, and changes in the fluorescence emission were evaluated by measuring the emission signal before and after the addition of the interfering ion at a 1.0×10^{-4} M final level to the Pb(II) solutions.

The relative error in the presence of the common interfering metal cations considered is less than $\pm 5\%$, which can be considered acceptable. Therefore, the presence of the other cations considered produces a negligible disturbance on the measurement of [Pb(II)] by the proposed optode, which can therefore be considered selective for this metal ion. Interestingly, the relative error in Figure 7 decreases following the decreasing order observed in the binding constants reported in Table 1 for the different metal cations considered.

3.7. Analytical Application

In order to investigate the potential use of the developed optical sensor for the determination of the Pb(II) concentration, it was applied to samples of canned tuna, prepared as described in Section 2.2.

The results for the Pb(II) content of the real samples determined by the proposed sensor (Table 3) nicely replicate those obtained via atomic absorption spectrometry (AAS).

Table 3. Results of three replicate determinations of the Pb(II) concentration using the developed sensor and AAS in different canned tuna samples.

Sample	Proposed Sensor/ppb	AAS/ppb	Relative Error (%)
1	92.77 ± 2.41	95.23 ± 2.63	2.58
2	115.84 ± 2.86	112.62 ± 2.47	2.86
3	86.92 ± 2.52	84.59 ± 2.28	2.75

3.8. Comparison

The overall performance of the proposed optical sensor was compared with that of recently reported Pb(II) optodes [16,48–53] (Table 4). The comparison highlights an overall higher performance in terms of the relatively short time to reach the equilibrium with the water solution of the analyte, low detection limit, and wide [Pb(II)] applicability range.

Table 4. Comparison of the parameters of the developed optode for Pb(II) determination with those of other recently reported Pb(II) optical sensor.

Measured Signal	Dynamic Range/M	Detection Limit/M	Response Time/Min	Ref.
Absorbance	8.05×10^{-8} – 2.24×10^{-5}	1.15×10^{-8}	7	[27]
Fluorescence	5.0×10^{-8} – 3.8×10^{-4}	2.2×10^{-8}	3	[48]
Absorbance	1.3×10^{-8} – 3.2×10^{-5}	9.0×10^{-9}	15	[49]
Absorbance	1.2×10^{-8} – 2.4×10^{-6}	4.0×10^{-9}	28	[53]
Fluorescence	3.0×10^{-7} – 2.5×10^{-2}	2.0×10^{-7}	5	[16]
Fluorescence	1.0×10^{-6} – 5.3×10^{-6}	5.3×10^{-7}	3	[50]
Fluorescence	6.0×10^{-9} – 4.1×10^{-5}	3.3×10^{-9}	1.5	[51]
Fluorescence	2.5×10^{-8} – 2.0×10^{-6}	1.0×10^{-8}	30	[52]
Fluorescence	1.0×10^{-9} – 1.0×10^{-3}	7.5×10^{-10}	3	This work

4. Conclusions

In this work, *N*-(3-(1,4-dioxo-7,13-dithia-10-azacyclopentadecan-10-yl)propyl)-5-(dimethylamino)naphthalene-1-sulfonamide (**L**) was considered as a fluorescent chemosensor for the development of a PVC-based optode for the detection of Pb(II) at a low concentration. **L** was designed according to the receptor–spacer–fluorophore supramolecular scheme by considering the mixed thio-oxa-aza macrocycle [15]aneNS₂O₂ as the receptor unit. In a MeCN solution, **L** shows the highest binding affinity for Pb(II), with the formation of 1:1 and 1:2 metal-to-ligand complex species (the structure of which was optimized at the DFT level), followed by Cd(II), Ag(I), and Hg(II). A decrease in the fluorescence emission intensity of **L** was observed in the presence of these four metal ions, with Pb(II) provoking the highest quenching effect. Once incorporated in plasticized PVC membrane in the presence of NaTPB, the optical selectivity of **L** toward Pb(II) increased significantly, with a very low influence on the fluorescence response exerted by competitive metal ions. Compared to other different optical sensors of Pb(II) reported in the literature, the optimized optode sensor featuring a PVC/NPOE/NaTPB/**L** wt% ratio of 30:60:5:5 resulted in a wide measuring range and a very low detection limit at pH = 5, following the fitting of the experimental data with Equation (6) and m:n = 1:1. Moreover, this optode sensor was successfully applied to determine the concentration of Pb(II) ions in real samples, with results that were in very good agreements with those obtained via atomic absorption spectrometry. Interestingly, both **L** and a similar fluorescent chemosensor featuring a [15]aneNS₂O₂ receptor unit linked to an *N*-(9-anthracenylmethyl)aminopropyl pendant arm [29], show a quenching effect only in the presence of Hg(II) for the former, and Hg(II) and Cu(II) for the latter in MeCN/H₂O (4:1 v/v) at pH = 7:0, while an insoluble precipitate is formed for both ligands in the presence of Pb(II) in this solvent mixture. Our results indicate that in MeCN and into a PVC–membrane, the complexation of Pb(II) with **L** can be studied and exploited for the preparation of a Pb(II)-selective optode for fluorimetric

measurements of Pb(II) in water solutions with little interference by the Hg(II) ion. In other words, despite in aqueous mixtures the complexation of Pb(II) by L results in the precipitation of insoluble complexes, which are useless from an analytical point of view, once incorporated within PVC membranes, L can be used for the analytical determination of Pb(II) in water solutions, adjusting the pH of the sample solution to 5.0. This clearly underlines the importance of the medium in which the host–guest interaction takes place, and supports the idea that within a conjugated fluorescence chemosensor built according to the receptor–spacer–fluorophore supramolecular scheme, both the receptor unit and the signaling unit can cooperate synergically in determining the optical and binding selectivity of the chemosensor, with the former not necessarily requiring the latter (for a more detailed discussion on this aspect, see ref. [11]). The optode described here presents a high applicative potentiality for the determination of Pb(II) in water solutions including real samples of this kind (such as rivers, lakes, and sea) without any specific pre-treatments of the real matrix other than adjusting the pH of the real matrix to 5.0. For the determination of Pb(II) in solid real samples, a sample pre-treatment is necessary to bring the target species in the water solution. In order to further develop the system in terms of portability, on-site possibility of determination of Pb(II), and easy-of-use devices, also in line with the new advanced “plug and play” optode configurations in similar fields [54–58], the optode proposed here features all the characteristics to be combined with computer screen photo-assisted technique (CSPT) devices, within chemical sensor arrays and multi-sensory platforms for toxic heavy metals [59–61].

Supplementary Materials: The following supporting information can be downloaded at: <https://www.mdpi.com/article/10.3390/chemosensors11120571/s1>, Figure S1: Plot of the fluorescence emission intensity versus time of the optode at the optimized composition for step changes in the concentration of Pb(II); Table S1: Results from thermochemical DFT calculations; Tables S2–S4: Optimized geometries in the gas phase in the orthogonal Cartesian format; Table S5: Imaginary and low-energy harmonic frequencies (cm^{-1}) calculated for L, $[\text{Pb}(\text{L})]^{2+}$ and $[\text{Pb}(\text{L})_2]^{2+}$ at DFT (mPW1PW/def2-SVP) in the gas phase.

Author Contributions: Conceptualization, M.S. and V.L.; methodology, M.S., V.L., M.A., M.M., A.G. and A.B.; Investigation, M.S., V.L., M.A., M.M., A.G. and A.B.; Supervision, M.S., V.L. and M.A.; data curations, M.S., V.L., M.A., M.M., A.G. and A.B.; writing—original draft preparation, M.S., V.L. and M.A.; Writing—review and editing, M.S., V.L., M.M., M.A., A.G. and A.B. All authors have read and agreed to the published version of the manuscript.

Funding: This research received no external funding.

Data Availability Statement: Data are contained within the article and supplementary materials.

Acknowledgments: The Razi University, Kermanshah (Iran), and The University of Cagliari (Italy) are acknowledged for financial support.

Conflicts of Interest: The authors declare no conflict of interest.

References

1. Aroua, M.K.; Leong, S.P.P.; Teo, L.Y.; Yin, C.Y.; Ashri, W.M.; Daud, W. Real-time determination of kinetics of adsorption of lead(II) onto palm shell-based activated carbon using ion selective electrode. *Bioresour. Technol.* **2008**, *99*, 5786–5792. [[CrossRef](#)] [[PubMed](#)]
2. Ghiaci, M.; Rezaei, B.; Kalbasi, R.J. High selective $\text{SiO}_2\text{-Al}_2\text{O}_3$ mixed-oxide modified carbon paste electrode for anodic stripping voltammetric determination of Pb(II). *Talanta* **2007**, *73*, 37–45. [[CrossRef](#)] [[PubMed](#)]
3. Vasimalai, N.; Abraham John, S. Spectrofluorimetric determination of picogram level Pb(II) using a dimercaptiothiadiazole fluorophore. *Spectrochim. Acta Part A Mol. Biomol. Spectr.* **2011**, *82*, 153–158. [[CrossRef](#)] [[PubMed](#)]
4. Arancibia, V.; Nagles, E.; Cornejo, S. Determination of lead in the presence of morin-5'-sulfonic acid and sodium dodecyl sulfate by adsorptive stripping voltammetry. *Talanta* **2009**, *80*, 184–188. [[CrossRef](#)] [[PubMed](#)]
5. Bispo, M.S.; Korn, M.D.G.A.; da Boa Morte, E.S.; Teixeira, L.S.G. Determination of lead in seawater by inductively coupled plasma optical emission spectrometry after separation and pre-concentration with cocrystallized naphthalene alizarin. *Spectrochim. Acta Part B Atomic Spectr.* **2002**, *57*, 2175–2180. [[CrossRef](#)]

6. Li, J.; Lu, F.; Umemura, T.; Tsunoda, K. Determination of lead by hydride generation inductively coupled plasma mass spectrometry. *Anal. Chim. Acta* **2000**, *419*, 65–72. [[CrossRef](#)]
7. Anthemidis, A.N.; Zachariadis, G.A.; Stratis, J.A. On-line preconcentration and determination of copper, lead and chromium(VI) using unloaded polyurethane foam packed column by flame atomic absorption spectrometry in natural water and biological samples. *Talanta* **2002**, *58*, 831–840. [[CrossRef](#)]
8. Cabon, J.Y. Determination of Cd and Pb in seawater by graphite furnace absorption spectrometry with the use of hydrofluoric acid as a chemical modifier. *Spectrochim. Acta Part B Atomic Spectr.* **2002**, *57*, 513–524. [[CrossRef](#)]
9. Fang, G.; Meng, S.; Zhang, G.; Pan, J. Spectrophotometric determination of lead in foods with dibromo-*p*-methyl-bromosulfonazo. *Talanta* **2001**, *54*, 585–589. [[CrossRef](#)]
10. Da Silva, A.P.; Gunaratne, H.Q.N.; Gunnlaugsson, T.; Huxley, A.J.M.; McCoy, C.P.; Rademacher, J.T.; Rice, T.E. Signaling Recognition Events with Fluorescent Sensors and Switches. *Chem. Rev.* **1997**, *97*, 1515–1566. [[CrossRef](#)]
11. Bencini, A.; Lippolis, V. Probing biologically and environmentally important metal ions with fluorescent chemosensors: Thermodynamic versus optical response selectivity in some study cases. *Coord. Chem. Rev.* **2012**, *256*, 149–169. [[CrossRef](#)]
12. Lodeiro, C.; Capelo, J.L.; Mejuto, J.C.; Oliveira, E.; Santos, H.M.; Pedras, B.; Nuñez, C. Light and colour as analytical detection tools; A journey into the periodic table using polyamines to bio-inspired systems as chemosensors. *Chem. Soc. Rev.* **2010**, *39*, 2948–2976. [[CrossRef](#)]
13. Lodeiro, C.; Pina, F. Luminescent and chromogenic molecular probes based on polyamines and related compounds. *Coord. Chem. Rev.* **2009**, *253*, 1353–1383. [[CrossRef](#)]
14. Shamsipur, M.; Hosseini, M.; Alizadeh, K.; Alizadeh, N.; Yari, A.; Caltagirone, C.; Lippolis, V. Novel fluorimetric bulk optode membrane based on a dansylamidopropyl pendant arm derivative of 1-aza-4,10-dithia-7-oxacyclododecane ([12]aneNS₂O) for selective subnanomolar detection of Hg(II) ions. *Anal. Chim. Acta* **2005**, *533*, 17–24. [[CrossRef](#)]
15. Shamsipur, M.; Alizadeh, K.; Hosseini, M.; Caltagirone, C.; Lippolis, V. A selective optode membrane for silver ion based on fluorescence quenching of the dansylamidopropyl pendant arm derivative of 1-aza-4,7,10-trithiacyclododecane ([12]aneNS₃). *Sens. Actuators B Chem.* **2006**, *113*, 892–899. [[CrossRef](#)]
16. Shamsipur, M.; Sadeghi, M.; Alizadeh, K.; Bencini, A.; Valtancoli, B.; Garau, A.; Lippolis, V. Novel fluorimetric bulk optode membrane based on 5,8-bis((5'-chloro-8'-hydroxy-7'-quinolinyl)methyl)-2,11-dithia-5,8-diaza-2,6-pyridinophane for selective detection of lead(II) ions. *Talanta* **2010**, *80*, 2023–2033. [[CrossRef](#)] [[PubMed](#)]
17. Prodi, L. Luminescent chemosensors: From molecules to nanoparticles. *New J. Chem.* **2005**, *29*, 20–31. [[CrossRef](#)]
18. Shamsipur, M.; Sadeghi, M.; Garau, A.; Lippolis, V. An efficient and selective fluorescent chemical sensor based on 5-(8-hydroxy-2-quinolinylmethyl)-2,8-dithia-5-aza-2,6-pyridinophane as a new fluoroionophore for determination of iron(III) ions. A novel probe for iron speciation. *Anal. Chim. Acta* **2013**, *761*, 169–177. [[CrossRef](#)]
19. Paderni, D.; Barone, G.; Formica, M.; Macedi, E.; Fusi, V. A novel 2,6-bis(benzoxazolyl)phenol macrocyclic chemosensor with enhanced fluorophore properties by photoinduced intramolecular proton transfer. *Dalton Trans.* **2023**, *52*, 3716–3724. [[CrossRef](#)]
20. Zhang, H.; Song, J.; Wang, S.; Song, Q.; Guo, H.; Li, Z. Recent progress in macrocyclic chemosensors for lead, cadmium and mercury heavy metal ions. *Dye. Pigment.* **2023**, *216*, 111380. [[CrossRef](#)]
21. Ding, Y.; Zhu, W.-H.; Xie, Y. Development of Ion Chemosensors Based on Porphyrin Analogues. *Chem. Rev.* **2017**, *117*, 2203–2256. [[CrossRef](#)] [[PubMed](#)]
22. Prodi, L.; Bargossi, C.; Montalti, M.; Zaccaroni, N.; Su, N.; Bradshaw, J.S.; Izat, R.M.; Savage, P.B. An Effective Fluorescent Chemosensor for Mercury Ions. *J. Am. Chem. Soc.* **2000**, *122*, 6769–6770. [[CrossRef](#)]
23. Wong, J.K.-H.; Todd, M.H.; Rutledge, P.J. Recent Advances in Macrocyclic Fluorescent Probes for Ion Sensing. *Molecules* **2017**, *22*, 200. [[CrossRef](#)] [[PubMed](#)]
24. Paderni, D.; Giorgi, L.; Voccia, M.; Formica, M.; Caporaso, L.; Macedi, E.; Fusi, V. A New benzoxazole-Based Fluorescent Macrocyclic Chemosensor for Optical Detection of Zn²⁺ and Cd²⁺. *Chemosensors* **2022**, *10*, 188. [[CrossRef](#)]
25. Dos Santos Carlos, F.; da Silva, L.A.; Zanolrenzi, C.; Souza Nunes, F. A novel macrocycle acridine-based fluorescent chemosensor for selective detection of Cd²⁺ in Brazilian sugarcane spirit and tobacco cigarette smoke extract. *Inorg. Chim. Acta* **2020**, *508*, 119634. [[CrossRef](#)]
26. Formica, M.; Fusi, V.; Giorgi, L.; Micheloni, M. New fluorescent chemosensors for metal ions in solution. *Coord. Chem. Rev.* **2012**, *256*, 170–192. [[CrossRef](#)]
27. Galiński, B.; Wagner-Wysiecka, E. Pyrrole bearing diazocrowns: Selective chromoionophores for lead(II) optical sensing. *Sens. Actuators B Chem.* **2022**, *361*, 131678. [[CrossRef](#)]
28. Nolan, E.M.; Lippard, S.J. Tools and Tactics for the Optical Detection of Mercuric Ions. *Chem. Rev.* **2008**, *108*, 3443–3480. [[CrossRef](#)]
29. Aragoni, M.C.; Arca, M.; Bencini, A.; Blake, A.J.; Caltagirone, C.; Decortes, A.; Demartin, F.; Devillanova, F.A.; Faggi, E.; Dolci, L.S.; et al. Coordination chemistry of *N*-aminopropyl pendant arm derivatives of mixed N/S-, and N/S/O-donor macrocycles, and construction of selective fluorimetric chemosensors for heavy metal ions. *Dalton Trans.* **2005**, 2994–3004. [[CrossRef](#)]
30. *Official Methods of Analysis of the Association of Official Analytical Chemists*, 13th ed.; Association of Official Analytical Chemists: Washington, DC, USA, 1980; p. 399.
31. Koch, W.; Holthausen, M.C.A. *Chemist's Guide to Density Functional Theory*; Wiley-VCH: New York, NY, USA, 2001.

32. Frisch, M.J.; Trucks, G.W.; Schlegel, H.B.; Scuseria, G.E.; Robb, M.A.; Cheeseman, J.R.; Scalmani, G.; Barone, V.; Petersson, G.A.; Nakatsuji, H.; et al. *Gaussian 16, revision B.01*; Gaussian, Inc.: Wallingford, CT, USA, 2016.
33. Goch, M.; Lutter, M.; Pintus, A.; Schollmeier, D.; Arca, M.; Lippolis, V.; Jurkschat, K. Chelating Phosphorus—An O,C,O-Coordinating Pincer-Type ligand Coordinating P^{III} and P^V Centres. *Chem. Eur. J.* **2022**, *28*, e202201447. [[CrossRef](#)]
34. Adamo, C.; Barone, V. Exchange functionals with improved long-range behavior and adiabatic connection methods without adjustable parameters: The *m*PW and *m*PW1PW models. *J. Chem. Phys.* **1998**, *108*, 664–675. [[CrossRef](#)]
35. Weigend, F.; Ahlrichs, R. Balanced basis sets of split valence, triple zeta valence and quadrupole zeta valence quality for H to Rn: Design and assessment of accuracy. *Phys. Chem. Chem. Phys.* **2005**, *7*, 3297–3305. [[CrossRef](#)] [[PubMed](#)]
36. Wiberg, K.B. Application of the pople-santry-segal CNDO method to the cyclopropylcarbinyl and cyclobutyl cation and to bicyclobutane. *Tetrahedron* **1968**, *24*, 1083–1096. [[CrossRef](#)]
37. Reed, A.E.; Weinstock, R.B.; Weinhold, F. Natural population analysis. *J. Chem. Phys.* **1985**, *83*, 735–746. [[CrossRef](#)]
38. Dennington, R.D.; Keith, T.A.; Millam, J.M. *GaussView, version 6.0.16*; Semichem, Inc.: Shawnee Mission, KS, USA, 2016.
39. Schaftenaar, G.; Noordik, J.H. Molden: A pre- and post-processing program for molecular and electronic structures. *J. Comput. Aided. Mol. Des.* **2000**, *14*, 123–134. [[CrossRef](#)] [[PubMed](#)]
40. Banthia, S.; Samanta, A. A New Strategy for Ratiometric Fluorescence Detection of Transition Metal Ions. *J. Phys. Chem. B* **2006**, *110*, 6437–6440. [[CrossRef](#)] [[PubMed](#)]
41. Roy, P.; Dhara, K.; Manassero, M.; Banerjee, P. Synthesis, characterization and selective fluorescent zinc(II) sensing property of three Schiff-base compounds. *Inorg. Chim. Acta* **2009**, *362*, 2927–2932. [[CrossRef](#)]
42. Aragoni, M.C.; Arca, M.; Bencini, A.; Blake, A.J.; Caltagirone, C.; Danesi, A.; Devillanova, F.A.; Garau, A.; Gelbrich, T.; Isaia, F.; et al. Novel fluorescent chemosensors for heavy metal ions based on functionalized pendant arm derivatives of 7-anthracenylmethyl-1,4,10-trioxo-7,13-diazacyclopentadecane. *Inorg. Chem.* **2007**, *46*, 8088–8097. [[CrossRef](#)]
43. Desvergne, J.P.; Czarnic, A.W. (Eds.) *Chemosensors for Ion and Molecule Recognition*; Kluwer Academic Publishers: Boston, MA, USA, 1997.
44. Bakker, E.; Buhlmann, P.; Pretsch, E. Carrier-based ion-selective electrodes and bulk optodes. 1. General characteristics. *Chem. Rev.* **1997**, *97*, 3083–3132. [[CrossRef](#)]
45. Ertas, N.; Akkaya, E.U.; Atman, O.Y. Simultaneous determination of cadmium and zinc using a fiber optic device and fluorescence spectrometry. *Talanta* **2000**, *51*, 693–699. [[CrossRef](#)]
46. Singh, A.K.; Singh, R.P.; Saxena, P. Cobalt(II)-selective electrode based on a newly synthesized macrocyclic compound. *Sens. Actuators B Chem.* **2006**, *114*, 578–583. [[CrossRef](#)]
47. Rosatzin, T.; Bakker, E.; Suzuki, K.; Suzuki, K.; Simon, W. Lipophilic and immobilized anionic additives in solvent polymeric membranes of cation-selective chemical sensors. *Anal. Chim. Acta* **1993**, *280*, 197–208. [[CrossRef](#)]
48. Aksuner, N. Development of a new fluorescent sensor based on a triazolo-thiadiazin derivative immobilized in polyvinyl chloride membrane for sensitive detection of lead(II) ions. *Sens. Actuators B Chem.* **2011**, *157*, 162–168. [[CrossRef](#)]
49. Bualom, C.; Ngeontae, W.; Nitiyanontakit, S.; Ngamukot, P.; Imyima, A.; Tuntulania, T.; Aeungmaitrepirom, W. Bulk optode sensors for batch and flow-through determinations of lead ion in water samples. *Talanta* **2010**, *82*, 660–667. [[CrossRef](#)] [[PubMed](#)]
50. Nur, Y.; Rohaeti, E.; Darusman, L.K. Optical Sensor for the Determination of Lead(II) Based On Immobilization of Dithizone onto Chitosan-Silica Membrane. *Indones. J. Chem.* **2017**, *17*, 7–14. [[CrossRef](#)]
51. Karachi, N.; Azadi, O.; Razavi, R.; Tahvili, A.; Parsae, Z. Combinatorial experimental and DFT theoretical evaluation of a nano novel thio-dicarboxaldehyde based Schiff base supported on a thin polymer film as a chemosensor for Pb²⁺ detection. *J. Photochem. Photobiol. A Chem.* **2018**, *360*, 152–165. [[CrossRef](#)]
52. Peng, L.; Xi, Q.; Wang, X.; Kan, Y.; Jiang, J.; Yu, R. Determination of Lead(II) by a Nitrocellulose Membrane Fluorescent Biosensor Based on G-Quadruplex Changes. *Anal. Lett.* **2014**, *47*, 2341–2349. [[CrossRef](#)]
53. Zargoosh, K.; Farhadian Babadi, F. Highly selective and sensitive optical sensor for determination of Pb²⁺ and Hg²⁺ ions based on the covalent immobilization of dithizone on agarose membrane. *Spectrochim. Acta Part A Mol. Biomol. Spectr.* **2015**, *137*, 105–110. [[CrossRef](#)]
54. Zheng, W.-L.; Zhang, Y.-N.; Li, L.-K.; Li, X.-G.; Zhao, Y. A plug-and-play optical fiber SPR sensor for simultaneous measurement of glucose and cholesterol concentrations. *Biosens. Bioelectron.* **2022**, *198*, 113798. [[CrossRef](#)]
55. Gambino, F.; Cicatello, P.; Giaquinto, M.; Cusano, A.M.; Aliberti, A.; Micco, A.; Iele, A.; Iaccarino, E.; Ruvo, M.; Ricciardi, A.; et al. Lab on fiber nano-cavity integrated with charge responsive microgels for biosensing. *Sens. Actuators B* **2022**, *353*, 131149. [[CrossRef](#)]
56. Power, S.M.; Free, L.; Delgado, A.; Richards, C.; Alvarez-Gomez, E.; Briciu-Burghina, C.; Regan, F. A novel low-cost plug-and-play multi-spectral LED based fluorometer, with application to chlorophyll detection. *Anal. Methods* **2023**, *15*, 5474–5482. [[CrossRef](#)] [[PubMed](#)]
57. Yang, Z.; Albrow-Owen, T.; Cai, W.; Hasan, T. Miniaturization of optical spectrometers. *Science* **2021**, *371*, eabe0722. [[CrossRef](#)] [[PubMed](#)]
58. Ricciardi, A.; Crescitelli, A.; Vaiano, P.; Quero, G.; Consales, M.; Pisco, M.; Esposito, E.; Cusano, A. Lab-on-fiber technology: A new vision for chemical and biological sensing. *Analyst* **2015**, *140*, 8068–8079. [[CrossRef](#)] [[PubMed](#)]

59. Lvova, L.; Pudi, R.; Galloni, P.; Lippolis, V.; Di Natale, C.; Lundström, I.; Paolese, R. Multi-transduction films for Electronic Tongue applications. *Sens. Actuators B* **2015**, *207*, 1076–1086. [[CrossRef](#)]
60. Macken, S.; Di Natale, C.; Paolesse, R.; D'Amico, A.; Lundström, I.; Filippini, D. Towards integrated devices for computer screen photo-assisted multi-parameter sensing. *Anal. Chim. Acta* **2009**, *632*, 143–147. [[CrossRef](#)]
61. Potyrailo, R.A.; Morris, W.G.; Leach, A.M.; Sivavec, T.M.; Wisnudel, M.B.; Boyette, S. Analog Signal Acquisition from Computer Optical Disk Drives for Quantitative Chemical Sensing. *Anal. Chem.* **2006**, *78*, 5893–5899. [[CrossRef](#)]

Disclaimer/Publisher's Note: The statements, opinions and data contained in all publications are solely those of the individual author(s) and contributor(s) and not of MDPI and/or the editor(s). MDPI and/or the editor(s) disclaim responsibility for any injury to people or property resulting from any ideas, methods, instructions or products referred to in the content.